

Nanoscale

Accepted Manuscript



This is an *Accepted Manuscript*, which has been through the Royal Society of Chemistry peer review process and has been accepted for publication.

Accepted Manuscripts are published online shortly after acceptance, before technical editing, formatting and proof reading. Using this free service, authors can make their results available to the community, in citable form, before we publish the edited article. We will replace this *Accepted Manuscript* with the edited and formatted *Advance Article* as soon as it is available.

You can find more information about *Accepted Manuscripts* in the [Information for Authors](#).

Please note that technical editing may introduce minor changes to the text and/or graphics, which may alter content. The journal's standard [Terms & Conditions](#) and the [Ethical guidelines](#) still apply. In no event shall the Royal Society of Chemistry be held responsible for any errors or omissions in this *Accepted Manuscript* or any consequences arising from the use of any information it contains.

Cite this: DOI: 10.1039/c0xx00000x

www.rsc.org/nanoscale

Paper

Inkjet Printing of Flexible High-Performance Carbon Nanotube Transparent Conductive Films by "Coffee Ring Effect"

Allon Shimoni,^a Suzanna Azoubel^a and Shlomo Magdassi*^a

5 Received (in XXX, XXX) Xth XXXXXXXXXX 20XX, Accepted Xth XXXXXXXXXX 20XX

DOI: 10.1039/b000000x

Transparent and flexible conductors are a major component in many modern optoelectronic devices, such as touch screens for smart phones, displays, and solar cells. Carbon nanotubes (CNTs) offer a good alternative to commonly used conductive materials, such as metal oxides (e.g. ITO) for flexible electronics. The production of transparent conductive patterns, and arrays composed of connected CNT "coffee rings" on a flexible substrate poly(ethylene terephthalate), has been reported. Direct patterning is achieved by inkjet printing of an aqueous dispersion of CNTs, which self assemble at the rim of evaporating droplets. After post-printing treatment with hot nitric acid, the obtained TCFs are characterized by sheet resistance of 156 Ω sq⁻¹ and transparency of 81% (at 600nm), which is the best reported values obtained by inkjet printing of conductive CNTs. This makes such films very promising as transparent conductors for various electronic devices, as demonstrated by an electroluminescent device.

1. Introduction

Transparent conductive films (TCFs) are a major component in optoelectronic devices, such as touch screens, liquid crystal displays (LCDs), organic light emitting diodes (OLEDs), electroluminescent devices and solar cells. The demand for TCFs is continually growing, and according to Sun et al. this trend will continue to grow as we move towards flexible and printable TCFs ("plastic electronics")¹. Currently, most TCFs are based on transparent conductive oxides (TCOs), mainly indium tin oxide (ITO). TCOs have many disadvantages, such as high cost, durability, and lifetime issues. This is due to the brittle nature of TCOs, and the complex manufacturing process which includes photolithography and etching where patterning is required. These obstacles have triggered many efforts to develop alternatives for conventional TCOs².

Recently we published a review on the use of conductive nanomaterials for TCOs replacements such as metallic NPs, metallic NWs, CNTs and graphene nanosheets³. The main methods for producing TCFs from nanomaterials, are based on self-assembly⁴⁻⁶, rod coating^{7,8}, filtration^{9,10} and spin coating^{11,12}. CNTs are very suitable for flexible transparent conductors, since the individual CNT has very high conductivity and current carrying capacity, as well as excellent mechanical properties¹³. Furthermore, CNTs are now in abundance and their price is continuously dropping due to improvements in large scale synthesis processes. Hecht et al. mention in their review that CNTs provide a most promising and mature technology, compared to other nanomaterials designed to replace ITO as a transparent conductive material¹⁴.

In previous publications, several approaches have been reported

for the production of TCF using CNTs. Mirri et al. reported on the production of films by dip coating (sheet resistance (Rs)=100 Ω sq⁻¹, and transparency (T)=90%)¹⁵. Recently, Park et al. reported on TCF formation by spray coating (Rs=310 Ω sq⁻¹, T=81%)¹⁶, Jo et al. produced CNT TCF by spin coating (Rs=59 Ω sq⁻¹, T=71%)¹⁷ and De A. et al. produced films by filtration (Rs=80 Ω sq⁻¹, T=75%)¹⁸. However, all these production methods are not capable of direct patterning.

Several approaches have been use for the production patterned CNT TCFs such as direct laser interference patterning¹⁹, filtration coupled with transfer printing^{20,21} and electrophoretic deposition²².

Inkjet printing has unique advantages over other methods; it is suitable for large area flexible devices and roll-to-roll processes, it is a non-contact method and it enables direct patterning of transparent conductors without the need for additional processes such as lithography and etching. Up to now, there have been only few reports about CNT TCF by inkjet printing. Mustonen et al. used a composite ink made of functionalized, single-wall carbon nanotubes (SWCNTs) and poly(3,4-ethylenedioxythiophene)-poly(styrenesulfonate) (PEDOT-PSS), and achieved a film with sheet resistance of 1 K Ω sq⁻¹ and transparency of 70% after 30 layers²³. Lee et al. has recently reported on the use of inkjet printing of UV/ozone treated SWCNT, obtaining sheet resistance and transparency of 870 Ω sq⁻¹ and 80% respectively after 40 layers²⁴. To the best of our knowledge, and as mentioned recently by Tortorich et al. in his review on inkjet printing of CNT, there have been no reports on CNT TCF by inkjet that demonstrated both, good sheet resistance and good transparency²⁵.

Typically, conductive films can be composed of many deposited CNT layers, thus obtaining decreased sheet resistance. However,

since increasing the number of CNT layers causes a significant decrease in the transparency of the film²⁶, there is a need for innovative approaches to increasing the conductivity of CNT films, while at the same time retaining its high transparency.

In order to achieve this goal we used the well known coffee-ring effect. As explained by Deegan et al., when a droplet containing dispersed particles dries on a solid surface, the contact line between the drop and the substrate is pinned to its initial position and leads to a dense ring-like pattern along the perimeter^{27,28}. This phenomenon is usually undesirable and many studies have been conducted in order to understand and eliminate this effect^{29,30}. Previously, we utilized this effect for the fabrication of TCF of 2D ring arrays composed of silver nanoparticles³¹. Since the ring's width is only a few microns, the conductive lines are invisible and, therefore, can be utilized as a replacement for ITO. In this work we formed arrays of connected "coffee rings" composed of CNTs in order to obtain flexible TCFs. These arrays are obtained by inkjet printing of CNT dispersions onto polyethylene terephthalate (PET) films.

Previous reports have already shown the "coffee ring" effect with CNT dispersion. Majumder et al. showed suppression of "coffee rings" by sufficient rapid heating of spray coated CNT films³². Denneulin et al. investigated the formation of CNT rings by different CNT inks, and showed that using SWCNT-COOH/PEDOT-PSS ink leads to a more homogeneous CNT film³³. Both papers have presented ways to prevent the "coffee ring" effect, a well known problem in inkjet-printing. In this report we tackle this problem in an attempt to find a solution that will provide us with a technology for the production of patterned CNT-TCF on polymeric substrates for application in the field of plastic electronics.

2. Results and Discussion

2.1 Single rings

Preliminary experiments were performed, in which we changed several ink and printing parameters, in order to study the formation of CNT rings by the coffee stain effect. Picoliter droplets of CNT dispersions were inkjet printed on a heated PET substrate. Each printed droplet formed a ring pattern in which the CNTs were mainly located on the ring's rim, leaving an empty space in the center (Figure 1). It should be noted that one of the advantages of the inkjet printing method is the reproducibility of the printed pattern, as seen by the uniform sizes of these rings.

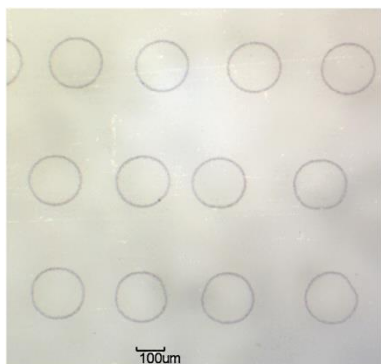


Fig. 1 Optical microscope image of CNT rings formed by inkjet printing. The uniformity of the rings can be observed.

In order to study the morphology of the pattern, mechanical and optical profilometer measurements were performed in the CNT rings (Figure 2). The results show that an edge of about 300nm in height is formed around the ring, placing most of the CNTs at the perimeter of the ring and leaving almost an empty hole in the center.

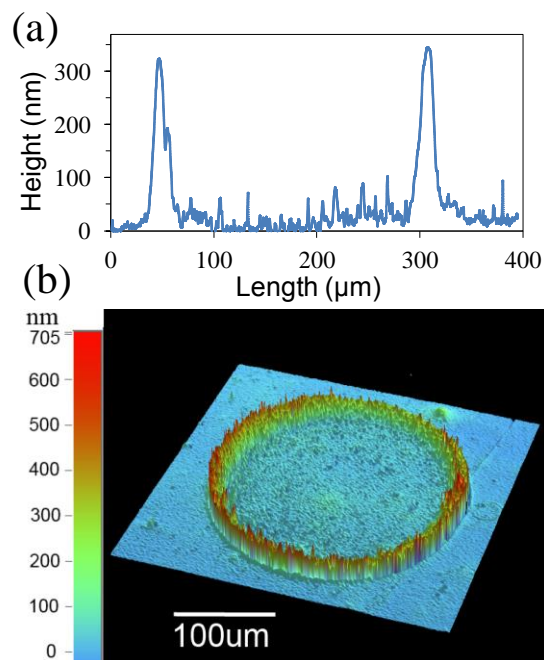


Fig. 2 Height profile of a CNT ring printed on PET, heated to 50°C and measured by (a) mechanical profilometer, (b) optical profilometer. The height of the ring was found to be about 300 nm, while the inside remained empty.

In order to obtain a 2D array of interconnected rings, a study of the parameters which affect the size of the individual rings, was performed. First, we investigated the effect of the substrate temperature on the ring's morphology. It was found that as the temperature increases, the ring's diameter decreases, as shown in Figure 3. This result can be explained by the faster pinning of the contact line upon contact of the droplet with the substrate, at higher temperature due to solvent evaporation. This can be also attributed to the evaporation rate close to the contact line which is faster than the deposition rate of the CNT as the temperature is increased.

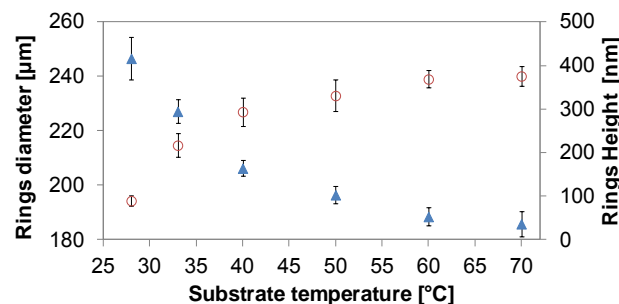


Fig. 3 The effect of substrate temperature on the ring's diameter and height. (▲ - diameter, ○ - height). As the temperature increases the diameter of the ring decreases from about 250 μm to 190 μm at 70°C. On the other hand the rings height increase from 90 nm at room temperature to 375 nm at 70°C.

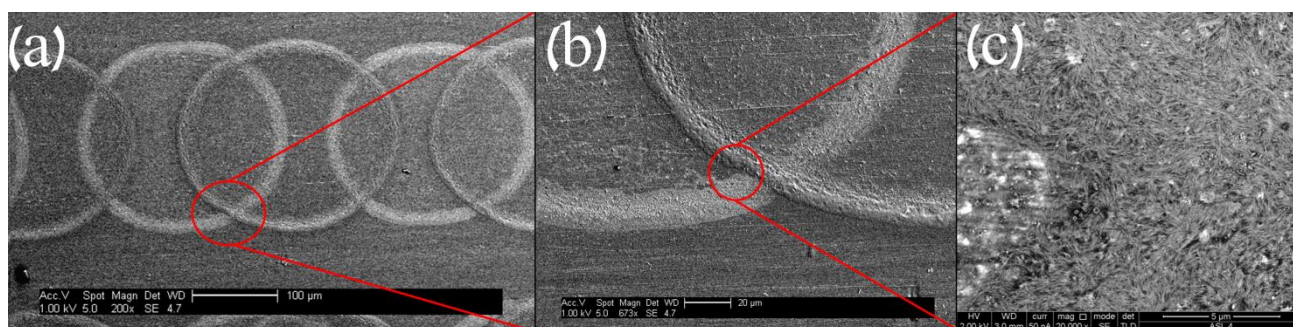


Fig. 4 HRSEM and EHRSEM images of connected rings. The connection between CNTs of different rings is similar to the connection between CNTs of the same ring.

At room temperature, the diameter of the ring was about 250 microns, while at 70°C it decreased to 190 microns. Obviously, since there is no CNT degradation at those temperatures, the increase in temperature should raise the height of the ring. When the substrate is at room temperature, the ring's height is about 90 nm, and increases to 375 nm when the substrate is heated to 70°C.

In further experiments the temperature of the substrates was set to 50°C, enabling rings with a mean diameter of about 200 μm, in which the effect of the temperature was already less significant, to print uniformed rings.

2.2 Connected rings

Once the printing resulted in reproducible individual rings, the second step was to connect rings to each other in order to provide a good percolation path in a 2D array.

As shown in Figure 4a and 4b, we found that interconnected rings can be obtained by printing a second layer of rings. This is done after cleaning the printed area, in between each layer with ethanol, in order to wash away excess surfactants from the ring's surface. The excess surfactant increases the substrate's hydrophilicity, thus preventing the formation of new rings. In order to confirm the connection in the junctions between the overlapping rings we performed HR SEM imaging, and as can be seen in Figure 4c the junction shows a homogenous area of CNTs between the two rings.



Fig. 5 Flexible CNT TCF formed by inkjet-printed CNT rings.

2.3 HNO₃ post-treatment

By printing several layers of connected rings onto each other with a slight shift in drop position at each layer, it was possible to obtain transparent films on a flexible PET substrate, as shown in Figure 5.

However, these films have high resistance (above 80 kΩ sq⁻¹). In order to obtain conductive films we performed post-treatment by dipping the film in nitric acid, as had been reported by several researchers. Geng et al. reports that the effect of HNO₃ post-

treatment is mainly due to the removal of the dispersant³⁴. Shin et al. reports that the nitric acid causes doping of the CNTs which decreases sheet resistance³⁵. However, there are no disagreements as to the benefit of such post-treatment. We found that post-treatment performed at various temperatures of HNO₃ solution had a tremendous effect on the sheet resistance of CNT TCF. When we dipped a 2D-ring array film with a transmittance of 82% (with 6 layers of rings, as described below), into HNO₃ solution at room temperature, we achieved a sheet resistance of 2500 Ω sq⁻¹. Increasing the temperature to 80°C improved the sheet resistance by over 50% and decreased it to 1080 Ω sq⁻¹ (Figure 6).

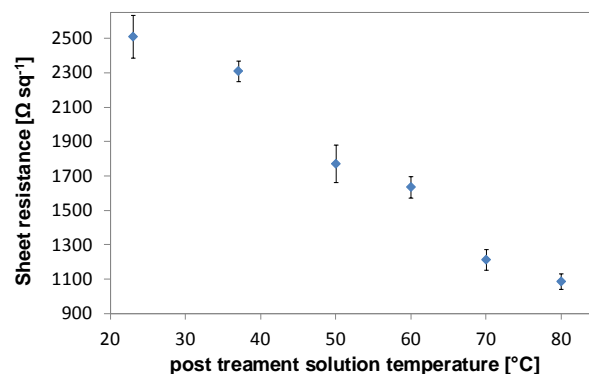


Fig. 6 Effect of HNO₃ solution temperature on sheet resistance. There is a clear decrease in sheet resistance as the acid temperature increases. The sheet resistance of 6 layers of rings with about 82% transparency decreased from 2500 Ω sq⁻¹ at room temperature to 1080 Ω sq⁻¹ at 80°C - an improvement of 57%.

Temperature is a key parameter due to the washing and doping reactions that occur during treatment. It should be mentioned that we limited the experiments to temperatures up to 80°C, since above that the PET becomes brittle and measurements cannot be performed. At 70°C, although measurements could be done, there was a slight distortion in the PET film, and therefore we decided to continue the experiments at 60°C.

2.4 Printed films

It was found that the number of printed layers affects sheet resistance and transmittance. As seen in Figure 7, the sheet resistance and transmittance of the film decreases as the number of printed layer increases. We printed films with up to 12 layers of rings and found an almost linear correlation between the sheet resistance and the numbers of printed layers - from 6 to 12 printed layers - as could be expected from adding a conductive

material into a conductive layer. The deviation from linearity of the 4-layered film can be explained by the fact that the rings are not fully connected and, therefore, lead to high sheet resistance. This is due to the inaccuracy of movement of our X-Y printing table, which leads to undesired shifts in placement of the droplets, leading to more random appearance.

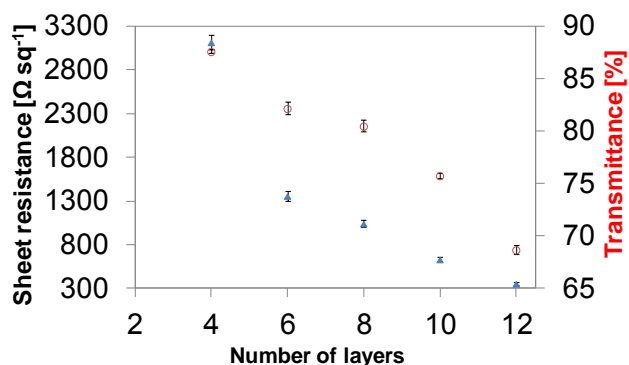


Fig. 7 Effect of the number of printed layers on sheet resistance and transmittance (▲ - sheet resistance, ○ - transmittance). As the number of layers increase both transparency and sheet resistance decrease from $T=87\%$ and $R_s=3120 \Omega \text{ sq}^{-1}$ for 4 layers, to $T=68\%$ and $R_s=350 \Omega \text{ sq}^{-1}$ for 12 layers.

It should be noted that the obtained sheet resistance results were not very low, which could be due to the inherent properties of the CNTs used in the above experiments. It is well known that different CNTs have different optoelectronic performance capabilities, mainly characterized by the I_G/I_D ratio of the Raman spectra^{36,37}. The CNTs used so far had an I_G/I_D ratio of 17. Therefore, a similar experiment was performed with other CNTs (ASP-100F SWCNTs from Hanwha Chemical) with an I_G/I_D ratio of 80. It was found that by using these CNTs a much lower sheet resistance was obtained, $156 \pm 13 \Omega \text{ sq}^{-1}$, and transparency of $81.4 \pm 0.1\%$ for 6 layers of CNT rings. The previous CNTs with about the same transparency ($82.2 \pm 0.6\%$) had sheet resistance of $1359 \pm 56 \Omega \text{ sq}^{-1}$. As mentioned above, the best performance of inkjet-printed CNTs TCF achieved up till now was sheet resistance of $870 \Omega \text{ sq}^{-1}$ and transparency of 80% after 40 layers. In this work we achieved sheet resistance of $156 \Omega \text{ sq}^{-1}$ for 81% transparency after only 6 layers.

In order to ascertain the advantage of 2D ring structure designed to achieve TCF, a comparative experiment was performed, in which a continuous layer of CNTs was inkjet-printed. To avoid ring formation the concentration of the wetting agent (Byk 348) in the CNT ink was increased to 1%. For $80.5 \pm 0.2\%$ transmittance the sheet resistance of the homogeneous films was $298 \pm 19 \Omega \text{ sq}^{-1}$, while with 2D ring structure we achieved $156 \pm 13 \Omega \text{ sq}^{-1}$ at a slightly better transparency of $81.4 \pm 0.1\%$, an improvement of 48%.

A major advantage of the proposed method is that it enables direct fabrication of patterned electrodes, as shown in Figure 8. This direct printing method is scalable, cost-effective, and could be utilized in broad electronic applications, such as touch screens of smart phones that require patterning which is typically achieved by an expensive, and a multi-step method such as lithography.

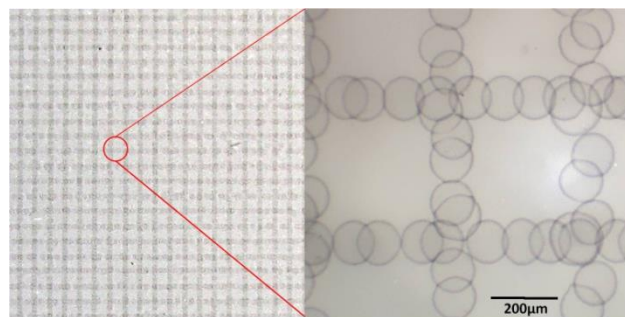


Fig. 8 Patterned grid made of CNTs rings.

2.5 EL device

TCF films, produced by inkjet printing CNT rings, remained stable for at least 3 months without any significant increase in sheet resistance. Since the 2D arrays were printed on top of a PET substrate, the flexibility of the PET and CNT rings' film, which have excellent adhesion and passed a scotch test with ASTM standard tape test, provided an excellent option for "plastic electronic" devices. We have demonstrated this concept by producing a flexible electroluminescent (EL) device using the 2D ring array. The device was prepared by printing 8 layers of CNT rings, as described above for the transparent electrode. The EL paste was screen-printed, and a full line of the CNT dispersion was inkjet printed (without rings) on top of the EL paste, as the counter electrode. As seen in Figure 9, it should be noted that the bending of the EL, up to an angle of 180° , does not affect the conductivity of the electrodes nor the luminance emitted by the device.

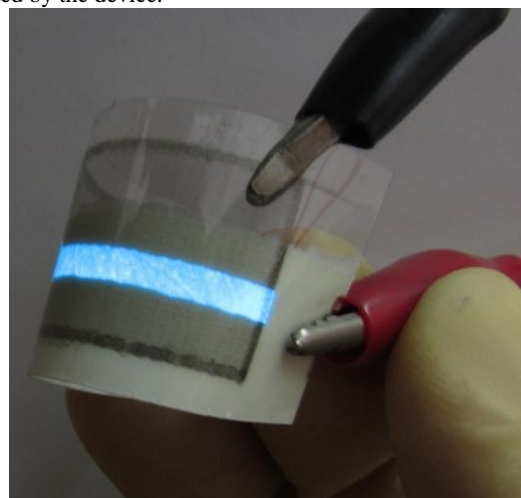


Fig. 9 Flexible EL device formed by transparent electrode made of inkjet-printed CNT rings.

3. Experimental section

3.1 Materials

SWCNTs of 0.7-1.4 nm diameter made by Chemical vapor deposition (CVD) were purchased from Sigma Aldrich, and SWCNTs Hanos ASP-100F made by arc-discharge were purchased from Hanwha Chemical and used as received. 0.1 wt% SWCNT was dispersed in a solution containing polymeric dispersant SOLSPERSE 46000 (1.5 wt%) (Lubrizol), and wetting

agent Byk 348 (0.2 wt%) (Byk-Chemie GmbH) in triple distilled water. The dispersion was prepared using a horn sonicator (model Vibra-Cell, Sonics & Materials) for 15 min, at 750 W, while cooling in an ice bath. The dispersion was then centrifuged at 3000 rpm for 15 min, and the supernatant was decanted. In comparative experiments intended to prevent the "coffee rings effect" we increased the wetting agent Byk 348 concentration to 1 wt%.

3.2 Printing of rings

The inkjet printing of the dispersions was performed by a Microfab JetDrive III printer with a 60 μm wide single nozzle. The parameters of the double waveform for all the printing experiments were: voltage - 70 V; frequency - 40 Hz; rise time - 3 μs ; dwell time - 30 μs ; fall time - 3 μs ; echo time - 35 μs ; and final rise - 3 μs . The movement of the substrate was controlled by a DMC-21x3 XY table (Galil Motion Control, Inc.). The substrate temperature was set to 25-70°C by Peltier heater/cooler, and the humidity within the printing chamber was fixed to 20-35% RH. The substrates used were polyethylene terephthalate - PET (Jolybar) precleaned with ethanol. After each layer the films were cleaned with ethanol before printing the next layer of rings. In order to achieve a conductive 2D array of rings, an overlapping of the rings is required. This was achieved by printing first layer of separated rings with a spacing of half the diameter of the ring, and second layer by repeating the same, with a shift of half ring. This enabled placing the second layer of the rings on top of two separated rings, thus enabling connectivity. The patterns were repeated in the X and Y direction, thus forming a 2D array of connected rings.

3.3 Film treatment

The post treatment was performed by dipping the samples for 10 minutes in a bath containing 70% HNO_3 solution (Bio Lab) at various temperatures, while stirring.

3.4 EL device

An electroluminescent (EL) device was fabricated as follows: Interconnected ring were printed and self-assembled on PET and the EL layers were screen-printed on top of it. The EL layer is composed of one layer of ZnS paste (Type E80-01EL, MOBIChem Scientific Engineering) and two layers of BaTiO_3 paste (Type D80-01, MOBIChem Scientific Engineering). The samples were dried at 120°C after each layer. The counter electrode was also prepared by inkjet printing the CNT dispersion (in several layers) on top of the EL layer.

3.5 Characterization

SEM images were performed by using high resolution scanning electron microscope (HR SEM) Sirion (FEI Company) and Extra High Resolution SEM (EHRSEM) Magellan 400 (FEI Company). The profiles of the rings were measured by a mechanical profilometer Dektak 150 Surface Profiler (Veeco) and by an optical profilometer ContourGT-I (Bruker). The sheet resistances were measured by a 4-point probe (Cascade Microtech) together with a milliohm meter (380562 model, Exteck instruments). The light transmittance of the films was measured at 600 nm, using a UV-vis spectrophotometer (Cary 100 model, Varian). Raman spectras were collected by using an inVia Raman microscope

(Renishaw) with excitation wavelength of 514 nm. The adhesion test was performed by using a ASTM standard tape test (Elcometer). The tape was observed visually and the resistivity was measured before and after the peeling test. No change and no visual difference indicate excellent adhesion.

Conclusions

In conclusion, a TCF with ~80% transparency and ~150 Ωsq^{-1} sheet resistance was printed by direct inkjet, allowing direct patterning. The patterned rings' dimensions could be controlled by the substrate temperature, enabling the control of the dimensions and the resolution of the chosen pattern. High transparency was obtained by inkjet printing of individual rings one on top of the other, which enabled multiple layers without major decrease in transparency. Low sheet resistance was obtained due to post treatment with hot nitric acid, which resulted in an improvement of up to 2.5 times in sheet resistance. This post treatment can be applied to a variety of CNT conductive films. It should be mentioned that the ink used in this research was water-based, and is compatible with many plastics used in the industry. We believe that the new CNT-based TCF formed by inkjet printing of CNT rings array can be highly useful in printed electronics. Although the applicability of these films was demonstrated in constructing a flexible electroluminescent (EL) device, the process and materials reported here can also be utilized in other flexible optoelectronic applications, such as OLEDs, photovoltaic cells, displays and touch screens of smart phones, which require specific patterning of the transparent electrodes.

Acknowledgements

This work was supported by the Singapore National Research Foundation under the CREATE program: Nanomaterials for Energy and Water Management, and by the Israel National Nanotechnology Initiative.

Notes and references

- ^a *Casali Center for Applied Chemistry and the Center for Nanoscience and Nanotechnology, Institute of Chemistry, The Hebrew University of Jerusalem, 91904 Jerusalem, Israel.*
E-mail: magdassi@mail.huji.ac.il
1. J. Sun and R. Wang, in *Syntheses and Applications of Carbon Nanotubes and Their Composites*, ed. S. Suzuki, InTech, 2013, Ch 14, pp. 313-335.
 2. A. Kumar and C. Zhou, *Acs Nano*, 2010, **4**, 11-14.
 3. M. Layani, A. Kamyshny and S. Magdassi, *Nanoscale*, 2014, **6**, 5581-5591.
 4. T. Tokuno, M. Nogi, J. Jiu, T. Sugahara and K. Suganuma, *Langmuir*, 2012, **28**, 9298-9302.
 5. M. Layani and S. Magdassi, *Journal of Materials Chemistry*, 2011, **21**, 15378-15382.
 6. H. Shimoda, S. Oh, H. Geng, R. Walker, X. Zhang, L. McNeil and O. Zhou, *Advanced Materials*, 2002, **14**, 899-901.
 7. C. Liu and X. Yu, *Nanoscale Research Letters*, 2011, **6**.
 8. L. Hu, H. Kim, J. Lee, P. Peumans and Y. Cui, *Acs Nano*, 2010, **4**, 2955-2963.
 9. G. Eda, G. Fanchini and M. Chhowalla, *Nature nanotechnology*, 2008, **3**, 270-274.

10. S. De, T. Higgins, P. Lyons, E. Doherty, P. Nirmalraj, W. Blau, J. Boland and J. Coleman, *Acs Nano*, 2009, **3**, 1767-1774.
11. H. Becerril, J. Mao, Z. Liu, R. Stoltenberg, Z. Bao and Y. Chen, *Acs Nano*, 2008, **2**, 463-470.
12. D. S. Leem, A. Edwards, M. Faist, J. Nelson, D. D. C. Bradley and J. C. de Mello, *Advanced Materials*, 2011, **23**, 4371-4375.
13. L. Hu, D. Hecht and G. Gruner, *Chemical Reviews*, 2010, **110**, 5790-5844.
14. D. Hecht, L. Hu and G. Irvin, *Advanced Materials*, 2011, **23**, 1482-1513.
15. F. Mirri, A. Ma, T. Hsu, N. Behabtu, S. Eichmann, C. Young, D. Tsentelovich and M. Pasquali, *Acs Nano*, 2012, **6**, 9737-9744.
16. C. Park, S. W. Kim, Y.-S. Lee, S. H. Lee, K. H. Song and L. S. Park, *Journal of Nanoscience and Nanotechnology*, 2012, **12**, 5351-5355.
17. J. Jo, J. Jung, J. Lee and W. Jo, *Acs Nano*, 2010, **4**, 5382-5388.
18. S. De, P. Lyons, S. Sorel, E. Doherty, P. King, W. Blau, P. Nirmalraj, J. Boland, V. Scardaci, J. Joimel and J. Coleman, *Acs Nano*, 2009, **3**, 714-720.
19. M. Castro, A. Lasagni, H. Schmidt and F. Mucklich, *Applied Surface Science*, 2008, **254**, 5874-5878.
20. Y. Zhou, L. Hu and G. Gruner, *Applied Physics Letters*, 2006, **88**.
21. Z. Wu, Z. Chen, X. Du, J. Logan, J. Sippel, M. Nikolou, K. Kamaras, J. Reynolds, D. Tanner, A. Hebard and A. Rinzler, *Science*, 2004, **305**, 1273-1276.
22. M. Lima, M. de Andrade, C. Bergmann and S. Roth, *Journal of Materials Chemistry*, 2008, **18**, 776-779.
23. T. Mustonen, K. Kordas, S. Saukko, G. Toth, J. Penttilla, P. Helisto, H. Seppa and H. Jantunen, *Physica Status Solidi B-Basic Solid State Physics*, 2007, **244**, 4336-4340.
24. Y. Lee, S. Kim, K. Lee, N. Myung and Y. Choa, *Thin Solid Films*, 2013, **536**, 160-165.
25. R. P. Tortorich and J.-W. Choi, *Nanomaterials*, 2013, **3**, 453-468.
26. S. Azoubel, S. Shemesh and S. Magdassi, *Nanotechnology*, 2012, **23**.
27. R. Deegan, O. Bakajin, T. Dupont, G. Huber, S. Nagel and T. Witten, *Nature*, 1997, **389**, 827-829.
28. R. D. Deegan, *Physical Review E*, 2000, **61**, 475.
29. L. Cui, J. Zhang, X. Zhang, L. Huang, Z. Wang, Y. Li, H. Gao, S. Zhu, T. Wang and B. Yang, *ACS Appl. Mater. Interfaces*, 2012, **4**, 2775-2780.
30. J. Perelaer, P. Smith, C. Hendriks, A. van den Berg and U. Schubert, *Soft Matter*, 2008, **4**, 1072-1078.
31. M. Layani, M. Gruchko, O. Milo, I. Balberg, D. Azulay and S. Magdassi, *Acs Nano*, 2009, **3**, 3537-3542.
32. M. Majumder, C. Rendall, M. Li, N. Behabtu, J. A. Eukel, R. H. Hauge, H. K. Schmidt and M. Pasquali, *Chemical Engineering Science*, 2010, **65**, 2000-2008.
33. A. Denneulin, J. Bras, F. Carcone, C. Neuman and A. Blayo, *Carbon*, 2011, **49**, 2603-2614.
34. H. Geng, K. Kim, K. So, Y. Lee, Y. Chang and Y. Lee, *Journal of the American Chemical Society*, 2007, **129**, 7758-+.
35. D. Shin, J. Lee, Y. Kim, S. Yu, S. Park and J. Yoo, *Nanotechnology*, 2009, **20**.
36. B. Liu, C. Hsu and W. Wang, *Journal of the Taiwan Institute of Chemical Engineers*, 2012, **43**, 147-152.
37. Z. Li, H. Kandel, E. Dervishi, V. Saini, Y. Xu, A. Biris, D. Lupu, G. Salamo and A. Biris, *Langmuir*, 2008, **24**, 2655-2662.